

Fermi resonance structure in the CH vibrational overtones of CD₃CHO^{a)}

A. Amrein, H. Hollenstein, M. Quack, and R. Zenobi^{b)}

Laboratorium für Physikalische Chemie der ETH Zürich (Zentrum), CH-8092 Zürich, Switzerland

J. Segall^{c)} and R. N. Zare

Department of Chemistry, Stanford University, Stanford, California 94305

(Received 28 October 1988; accepted 1 December 1988)

Gas-phase fundamental and CH and CO overtone spectra (700–17 500 cm⁻¹) of 2,2,2-trideuteroacetaldehyde were recorded using FTIR and laser photoacoustic techniques. The Fermi resonance structure in the overtone spectra of the coupled CH stretching and in-plane CH bending vibrations is analyzed with a tridiagonal Hamiltonian, yielding a large effective coupling constant, $|k'_{sbb}| = 93 \text{ cm}^{-1}$, corresponding to subpicosecond redistribution times. No coupling between the out-of-plane CH bending mode and the Fermi resonance system is apparent. This study presents the first detailed analysis of the anharmonic couplings in the CH chromophore at an sp² carbon atom. The in-plane CH bending vibration couples in a manner similar to the CH(sp³) bending vibrations, whereas the out-of-plane bending vibration is decoupled, similar to the CH(sp) bending vibrations.

I. INTRODUCTION

Fermi resonances¹ provide an essential mechanism for intramolecular vibrational energy flow² and often dominate the vibrational dynamics in highly excited molecules.³ In previous investigations, we have established an apparently universal existence of a strong Fermi resonance between CH stretching and bending vibrations in the sp³ alkyl CH chromophore.^{4–10} Because of the low CH bending frequencies in the acetylenic sp CH chromophore this resonance is quenched, which can be understood on the basis of an adiabatic separation between stretching and bending motions.^{4,11,12} The question arises, how the coupling in an sp² CH chromophore relates to the coupling in sp and sp³ CH chromophores. The nature of the sp² CH chromophore is of particular interest, because a Fermi resonance has been proposed¹³ to be partly responsible for the broad absorption features in room temperature benzene.¹⁴ However, recent spectra of jet cooled benzene¹⁵ may question this interpretation.

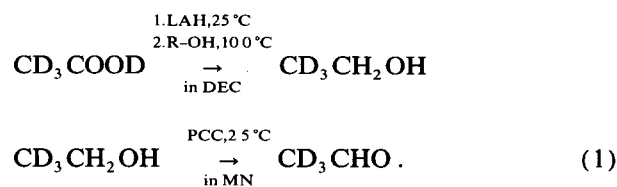
In order to investigate the Fermi resonance structure in the spectrum of the CH chromophore of sp² hydrocarbons we have selected trideuteroacetaldehyde (CD₃CHO) as one model system. The high overtone absorption in this compound is dominated by the isolated sp² CH chromophore with its coupled stretching and bending modes. A Fermi resonance doublet structure with bands at 2821 and 2719 cm⁻¹ has been found in the CH stretching fundamental. The in-plane bending fundamental is at 1388 cm⁻¹, whereas the out-of-plane bending fundamental was found at 624 cm⁻¹.¹⁶ Thus, there is the interesting possibility of a further 1:2 Fermi resonance between the two bending vibrations. The goal of our study was to characterize completely the high overtone spectra and to provide an analysis in terms of the various possible resonances. There have been no previous stud-

ies of the overtone spectra of this compound but there exist two recent investigations of the much more complex overtone spectra of CH₃CHO, which are dominated by the methyl group absorptions.^{17,18}

There is a fair amount of spectroscopic ground work available for acetaldehyde and its isotopomers.^{16–24} In particular, Kilb *et al.*¹⁹ have determined structural and torsional properties, Bauder *et al.*²⁴ have critically reviewed the microwave literature, and Hollenstein and Günthard¹⁶ have presented a normal coordinate analysis. In the latter work, the existence of a stretch bend Fermi resonance in the fundamental region was already established, which provided one reason for selecting CD₃CHO for a more detailed study of the overtone spectra.

II. EXPERIMENTAL

Large amounts of CD₃CHO were necessary for recording the overtone spectra. Starting from commercially available perdeuterated acetic acid, CD₃COOD was synthesized according to the following scheme:



The reduction in the first step was performed with LiAlH₄ (LAH) using diethyleneglycolmonomethylether, CH₃O(CH₂)₂O(CH₂)₂OH, (ROH), to hydrolyze the initially formed aluminum complex [(CD₃CH₂O)₄Al]⁻Li⁺ and diethyleneglycoldiethylether,



as solvent with high boiling point (189 °C). The oxidation in the second step was carried out with pyridinium-chloromono-chromate (deuteriochloride, PCC) in 1-methylnaphthalene as solvent (MN, boiling point 244 °C). The deuteriochloride of PCC was chosen as a reactant to prevent possible proton exchange of the α-deuteriums in the acidic medium of the

^{a)} From: Renato Zenobi, Diplomarbeit, ETH Zürich (1986).

^{b)} Present address: Department of Chemistry, Stanford University, Stanford, California 94305.

^{c)} Present address: Department of Chemistry, University of Southern California, Los Angeles, California 90089.

second step. The procedure allows easy separation of the intermediate trideuteroethanol by distillation, and of the product trideuteroacetaldehyde by pumping off at 15 mbar. All reactions were carried out under dry N₂ in order to avoid contamination with water. More than 0.5 mol of CD₃CHO could be synthesized with greater than 99.6% chemical purity and greater than 97.7% deuteration in the CD₃ group, as proven by gas chromatography, NMR spectroscopy, and IR spectroscopy. This also established the identity of the product. The sample preparation for quantitative spectroscopy included several freeze-pump-thaw cycles in order to remove air.

Using the Zürich BOMEM DA002 interferometric Fourier transform spectrometer system, which allows for a maximum apodized resolution of 0.004 cm⁻¹, several spectra were taken at modest resolution to cover the complete range from 700 to about 14 000 cm⁻¹. Selected regions were then measured at high resolution. The optical path in a multipass cell was calibrated using CHF₃ as a standard. Band strength measurements (pressure broadened spectra with 1 bar N₂) are estimated to be accurate within about 20% in the $N = 1$ and $N = 2$ overtone region and within about 40% in the $N = 3$ and 4 overtone spectra. The frequency measurement is accurate within the resolution as checked by several calibrations. Details of the techniques have been described extensively elsewhere.^{5,7}

The overtones in the visible have been measured in Stanford by the photoacoustic technique in the range from 12 000 and 17 500 cm⁻¹ using several laser dyes. Typical CD₃CHO pressures in these measurements were 500 mbar. Some samples in these measurements contained CO₂, which did not perturb the results, because the CO₂ absorption is very weak in this range. Band strengths were estimated using benzene and neopentane as internal references. However, this did not allow for a direct comparison with the FTIR data. Details of the Stanford photoacoustic laser spectroscopy system and experimental procedures have been described before.^{9,25,26}

III. RESULTS AND DISCUSSION

A. Rotational band shapes and fundamental spectrum in the mid infrared

CD₃CHO has C_s symmetry with the a and b principal axes in the plane of symmetry (coinciding with the CHO

TABLE I. Fundamentals of CD₃CHO.

	$\bar{\nu}(\text{cm}^{-1})$	Remarks and references
ν_1	2756.1	CH stretching ^a
ν_2	2262.2	CD ₃ stretching
ν_3	2120.24	CD ₃ stretching ^b
ν_4	1752(1754.33)	CO stretching ^b
ν_5	1395.3(1387.67)	in-plane CH bending ^c
ν_6	1131.4	CC stretching ^d
ν_7	1038.4	CD ₃ bending ^d
ν_8	961.03	CD ₃ bending ^d
ν_9	774.3	CC stretching ^{d,g}
ν_{10}	444	CCO bending ^d (Ref. 16)
ν_{11}	2225.14	CD ₃ stretching
ν_{12}	1061.8	CD ₃ bending ^{d,e}
ν_{13}	1027.5	CD ₃ bending ^{d,e}
ν_{14}	624	CH bending ^{d,f} (Ref. 16)
ν_{15}	(135)	torison (calculated) (Ref. 16)

^a From Fermi resonance analysis Ref. 16 estimates 2754 cm⁻¹.

^b The first value is from the overtone analysis, the fundamental is near 1754 cm⁻¹ in Fermi resonance with $\nu_8 + \nu_9$ at 1729.18 cm⁻¹, see Table V, contains some CH bending.

^c From Fermi resonance analysis, the value of the band center of the fundamental is given in parenthesis. The normal vibration contains some CO stretching.

^d Highly nonlocal, complex normal coordinate.

^e Some CH out-of-plane bending.

^f Also considerable CD₃ bending.

^g In Fermi resonance with $\nu_{14} + \nu_{15}$ at 723.63 cm⁻¹.

^h In Fermi resonance with $\nu_6 + \nu_8$ at 2084.4 cm⁻¹.

plane) and the c axis perpendicular to it. The a axis lies nearly along the line connecting the methyl carbon with the oxygen nucleus and thus CD₃CHO is a prolate, nearly symmetric top with rotational constants¹⁹ $A = 1.3920$ cm⁻¹, $B = 0.28652$ cm⁻¹, and $C = 0.26074$ cm⁻¹ (asymmetry parameter $\kappa = -0.954$). There are 10 a' (ν_1 to ν_{10}) and 5 a'' (ν_{11} to ν_{15}) normal vibrations. For a' fundamentals and overtones A , B , or AB hybrid bands are expected, whereas the a'' transitions should be of type C . Table I gives a summary of the fundamental frequencies of CD₃CHO and Fig. 1 provides a survey of the mid IR spectrum showing some of the fundamentals. We shall concentrate here on those vibrations relevant for the analysis of the overtone spectra. Our data for the whole range are in general agreement with previous results¹⁶ but more accurate. The data in Table I consist mainly of estimated band centers obtained without line by line rotational analysis.

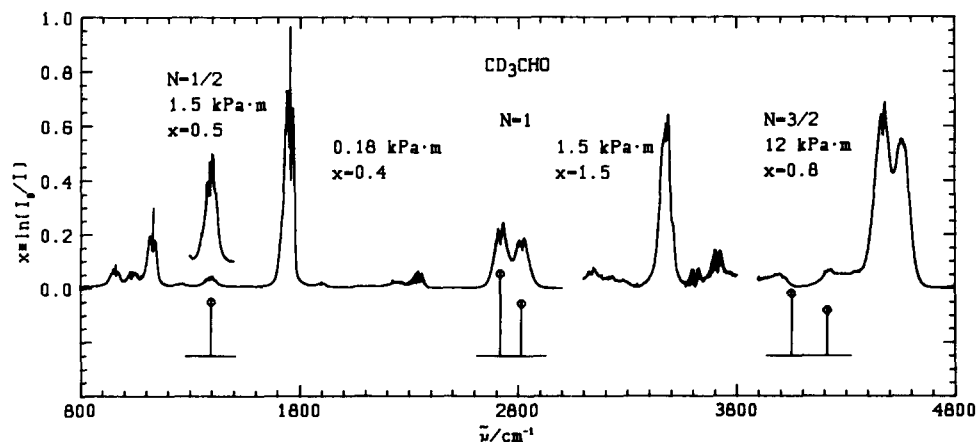


FIG. 1. Survey of the mid-infrared spectrum of CD₃CHO. Note the different conditions of measurement, which are indicated in the inserts as pressure times path length and scaling factor x for the ordinate. The sticks represent predicted band positions and intensities from the Fermi resonance analysis given below.

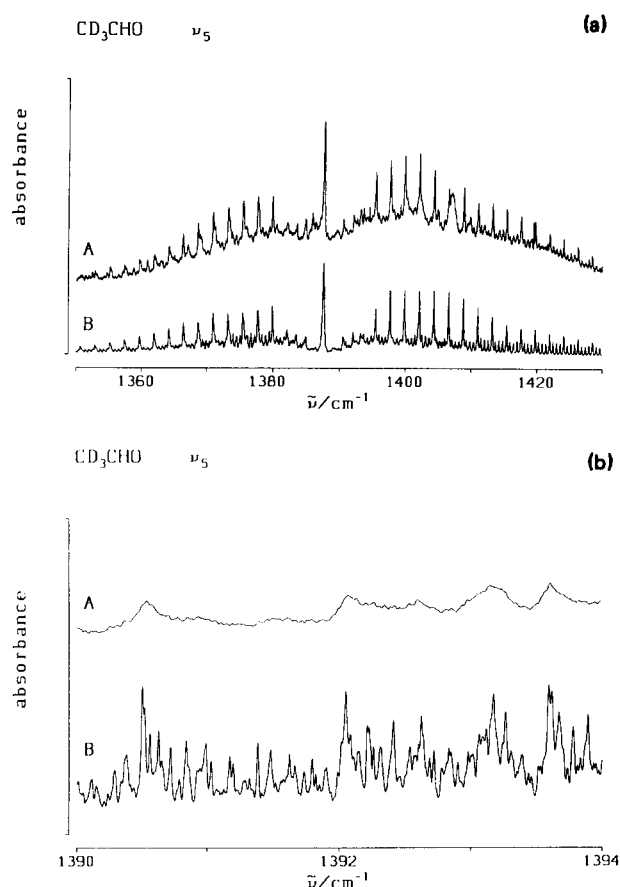


FIG. 2. High resolution scans of the in-plane CH bending fundamental (a) Survey at $p = 90$ mbar, $l = 17$ cm, apodized resolution 0.02 cm^{-1} (A = experiment, B = simulation with a Lorentzian pressure broadening of width FWHM of 0.1 cm^{-1}). (b) Detail showing the effect of pressure broadening [A: conditions of Fig. 2(a), B: $p = 5$ mbar, $l = 3.75$ m, apodized resolution 0.008] see also discussion in the text.

The in-plane CH bending fundamental ν_s (or ν_b) is a moderately strong band. A preliminary analysis of the high resolution spectrum gives a band center of 1387.67 cm^{-1} . Figure 2(a) shows a survey spectrum of this band obtained for a sample at a pressure of 90 mbar, in comparison with a simulated envelope based on preliminary spectroscopic constants and a pressure self-broadening coefficient of 1 $\text{cm}^{-1}/\text{bar}$. Figure 2(b) shows a comparison of a small section of this spectrum with a result obtained in a long path cell and 5 mbar sample pressure. This illustrates the surprisingly large pressure broadening in this band. The A:B ratio of this AB hybrid band was estimated from the simulation to be about 28:72. The CH in-plane bending motion is somewhat mixed with the CO stretching motion, which is of the same symmetry and rather close in frequency. From a purely local CH-bending mode a higher A content would have been expected. The CO-stretching fundamental appears very strongly at 1754 cm^{-1} (see Fig. 1). The CH stretching fundamental (ν_1 or ν_s) is in strong Fermi resonance with the first overtone of the CH bending vibration. This leads to the appearance of a doublet centered near 2750 cm^{-1} and the complex overtone spectrum, as discussed below in detail. Another vibration of potential importance for the CH overtone spectrum is the

out-of-plane CH-bending vibration. All normal vibrations of the triplet ν_{12} , ν_{13} , and ν_{14} contain a substantial amount of this local CH bending motion. If the fundamental at 624 cm^{-1} is associated with the out-of-plane bending motion, a Fermi resonance of its overtone near 1250 cm^{-1} with the in-plane bending vibration might perhaps be expected, and this resonance pair might be coupled to the CH stretching mode and fall closer to it at high overtones. As we shall see below, no evidence for such a behavior is found experimentally.

B. The evaluation of the CH stretch–bend resonance Hamiltonian and spectrum

By analogy to the sp^3 CH chromophore we might expect the CH overtone spectrum to be dominated by the CH stretching and bending vibrations, which are strongly coupled by anharmonic Fermi and Darling–Dennison resonances. The general theory for the asymmetric top cases has been outlined in Ref. 10. In the present case we found that the low frequency bending mode is decoupled. Consequently, the Fermi resonance occurs between the CH stretching mode ν_s and the high frequency in-plane CH bending mode ν_b . The effective Hamiltonian is block diagonal in the chromophore quantum number

$$N = \nu_s + 0.5\nu_b. \quad (2)$$

For integer N each block contains $N + 1$ coupled states, for half (odd) integer N one has $N + \frac{1}{2}$ states. The diagonal elements of the Hamiltonian matrix are given (in wave numbers) by Eq. (3):

$$H_{\nu_s, \nu_b, \nu_s, \nu_b}^N = \tilde{\nu}'_s \nu_s + \tilde{\nu}'_b \nu_b + x'_{ss} \nu_s^2 + x'_{bb} \nu_b^2 + x'_{sb} \nu_s \nu_b. \quad (3)$$

The nonzero off-diagonal elements in each block are given by Eq. (4)

$$H_{\nu_s, \nu_b, (\nu_s - 1), (\nu_b + 2)}^N = \frac{1}{2} k'_{sbb} [0.5\nu_s (\nu_b + 1) (\nu_b + 2)]^{1/2}. \quad (4)$$

The effective Hamiltonian is defined by six spectroscopic parameters, for which we have used conventional symbols supplemented by a prime. The parameters have a complex significance. To lowest order, the off-diagonal Fermi resonance parameter k'_{sbb} can be associated conventionally with a cubic force constant in the normal coordinate (q) representation of the potential, corresponding to the term $k_{sbb} q_s q_b^2$.²⁷ This is a very rough approximation, which is now known to be poor, in general, and more fundamental interpretations have been discussed elsewhere.^{5–7} The eigenvalues of the effective Hamiltonian can be compared to the positions of overtone bands in the CH spectrum. The eigenvector components can be used to calculate relative intensities within the polyads. If one assumes that only the pure CH stretching overtones carry oscillator strength one has for the relative band strengths g_{N_j} :^{5–7}

$$Z_N^T H^N Z_N = \text{Diag}\{E_1^N, E_2^N, \dots\} \quad (5)$$

$$g_{N_j} = |Z_{N1j}|^2, \quad (6)$$

$$\sum_j g_{N_j} = \sum_j |Z_{N1j}|^2 = 1. \quad (7)$$

Relative band strengths can also be obtained from experiment using the relations:

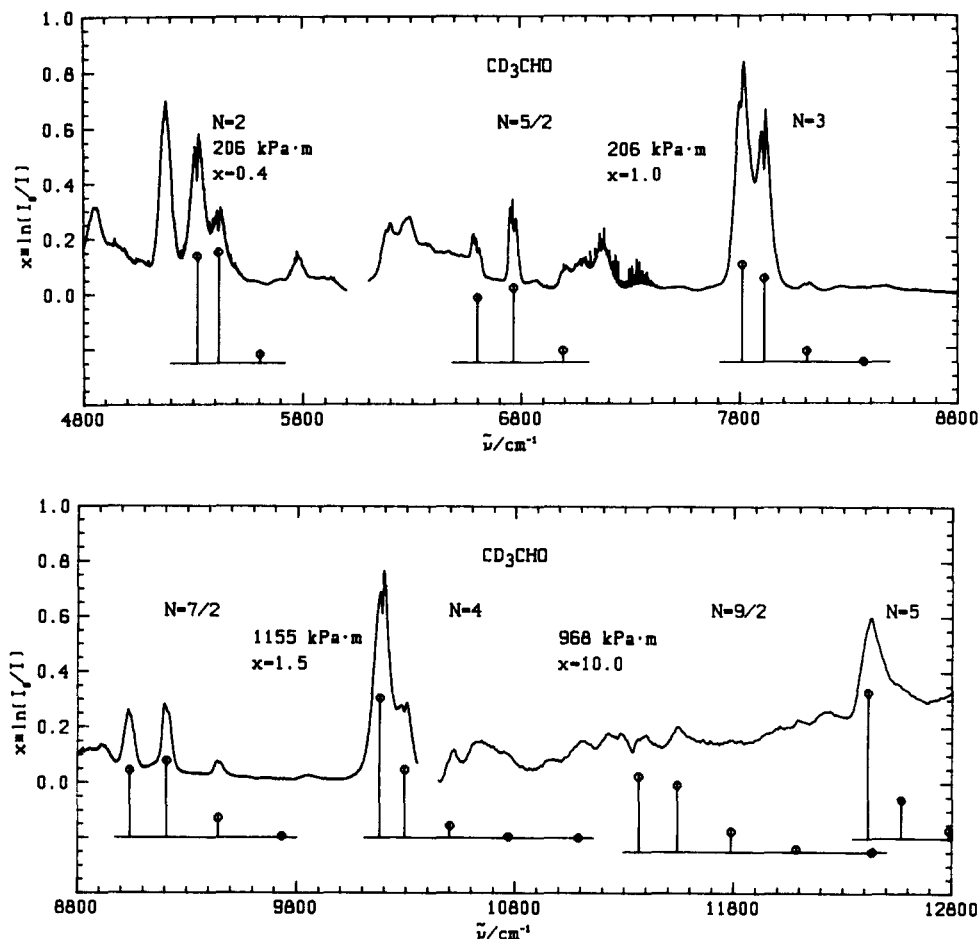


FIG. 3. Survey of the (FTIR) near infrared spectrum of CD₃CHO (see also caption in Fig. 1 and discussion in the text). The sticks represent predicted band positions and intensities from the Fermi resonance Hamiltonian.

$$g_{N_j}^{\text{exp}} = G_{N_j}^{\text{exp}} / \sum_j G_{N_j}^{\text{exp}} \quad (8)$$

$$G_{N_j}^{\text{exp}} = \int_{\text{band } N_j} \sigma(\tilde{\nu}) \left(\frac{d\tilde{\nu}}{\tilde{\nu}} \right) \approx \frac{1}{\tilde{\nu}_0 C l} \int_{\text{band } N_j} \ln \left(\frac{I_0}{I} \right) d\tilde{\nu}. \quad (9)$$

The sums in these equations are taken over the states in each polyad N . N_j labels states in the polyad N in the order of decreasing energy with increasing j . The absorption cross section σ , the band center $\tilde{\nu}_0$, particle density concentration C , optical absorption path length l , and incident (I_0) and transmitted (I) intensity have their usual significance. Deviations from the simple one-dimensional dipole function model for low overtones are expected. We shall see later that deviations also occur for some of the higher overtones. They can be understood qualitatively and thus only *approximate* agreement of experimental and theoretical intensities should be expected. Nevertheless, the relative intensities are crucial for the Fermi resonance band assignments. They are the signature of the CH chromophore in the spectrum.

C. The CH chromophore overtone spectra

Figures 3 and 4 provide a survey of the complete near infrared and visible spectra of CD₃CHO up to about 17 500 cm^{-1} . The CH overtone bands have been assigned by means of the effective Hamiltonian in Sec. III B. After a nonlinear least square fit using the Marquardt algorithm in a program

developed previously,¹⁰ one can predict band positions (sticks) and intensities (relative heights of the sticks) which are shown in the figures. Nevertheless, the Fermi resonance polyads for integer and half (odd) integer N in Figs. 3 and 4 are easily recognized. The absolute intensities are, of course, quite different in the different ranges (see the conditions given in the figures and captions). Because of the large anharmonicity of the CH stretching mode, the lowest frequency band becomes increasingly dominant for large values of integer N . In the case of $N = 5$ there is some overlap between the FTIR and the photoacoustic spectra, with good agreement among the two. For the highest overtones the polyads are dominated by one or two intense bands. For most of the infrared bands, some coarse rotational structure is observed. We have not evaluated the rotational fine structure for most of the overtone bands, but we have estimated the band centers from the minima of resolved PQR structures and the central maxima for PQR structures. For the overtones in the visible, only the maxima of the moderately broad bands could be evaluated.

Table II summarizes the wavenumber and intensity information from experiment and theory. For such a simple model the fit is generally very good with a root mean square deviation of 4.4 cm^{-1} . The best fit parameters of the effective Hamiltonian are given in Table III. The large parameters are well determined and not very sensitive to details of the weighting or the fit procedure. This is evident, for instance,

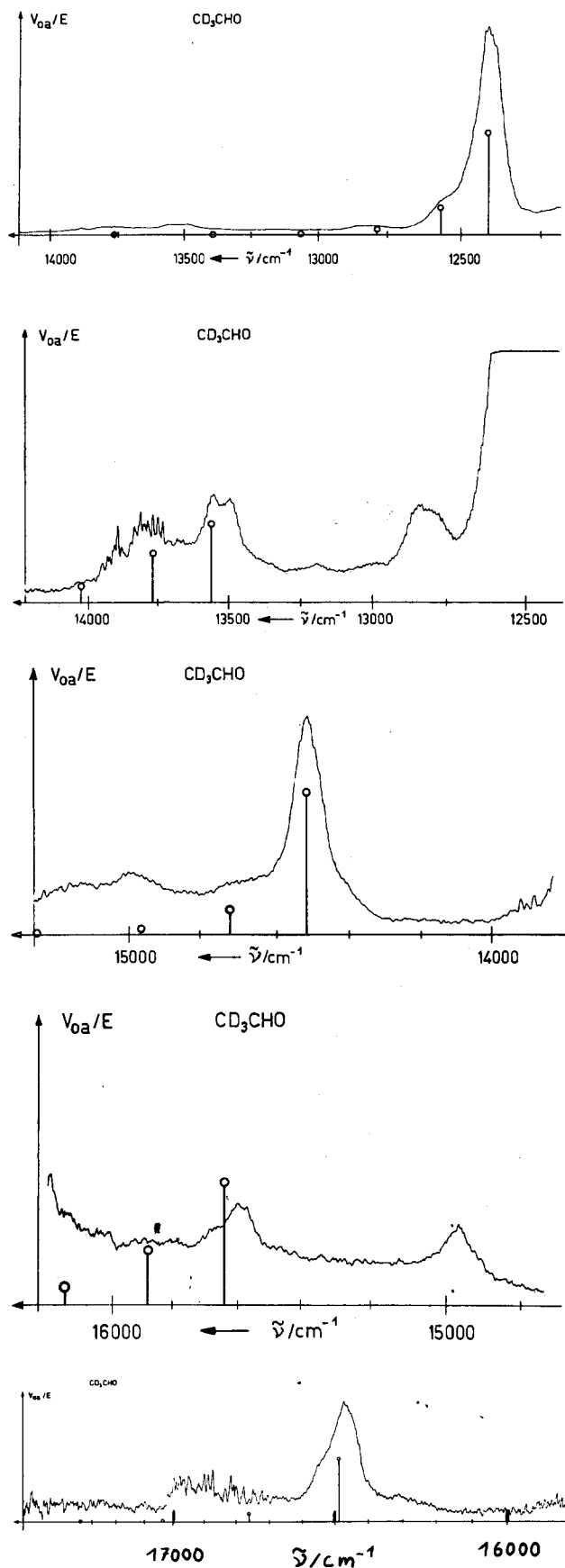


FIG. 4. Survey of the (photoacoustic) visible absorption spectrum of CD₃CHO (see also captions to Figs. 1 and 3, discussion in the text, and Sec. II for conditions). The ordinate gives the raw spectral signal which should be proportional to both absorption (1-transmittance) and absorbance [$\ln(I_0/I)$] for the weak signals.

TABLE II. Experimental and calculated^a results.

State	N	j	$\tilde{\nu}_j^{\text{obs}}(\text{cm}^{-1})$	$\tilde{\nu}_j^{\text{calc}}(\text{cm}^{-1})$	g_j^{obs}	g_j^{calc}	Weights ^c	Notes
	1/2	1	1 387.7	1 395.4		1.0	1.0	d
	1	1	2 821.0	2 814.2	0.46	0.390	1.0	d,e
		2	2 719.9	2 719.0	0.54	0.610	1.0	d,e
	3/2	1		4 213.8		0.421	...	f,(g)
		2		4 050.8		0.579	...	f,g
	2	1	5 614(?)	5 607.8	vw	0.038	...	g
		2	5 418.5	5 419.3	0.30	0.489	1.0	e,g,h
		3	5 321.8	5 322.2	0.66	0.473	1.0	e,g,h
	5/2	1	6 994	6 992.8	vw	0.078	1.0	g,i
		2	6 763	6 764.7	0.6	0.493	1.0	
		3	6 597	6 599.9	0.3	0.429	1.0	i
	3	1	...	8 368.3	...	0.003	...	f
		2	8 107.0	8 107.3	0.029	0.057	1.0(5.0)	
		3	7 911.1	7 911.4	0.402	0.435	1.0(1.0)	e
		4	7 807.2	7 811.0	0.566	0.505	1.0(1.0)	e
	7/2	1	...	9 733.7	...	0.010	...	
		2	9 446	9 442.3	0.084	0.119	1.0(2.0)	j
		3	9 207	9 207.5	0.507	0.465	1.0(1.0)	
		4	9 035	9 040.1	0.399	0.406	1.0(1.0)	j
	4	1	...	11 088.7	...	0.2(-3)	...	
		2	...	10 768.8	...	0.005	...	
		3	10 501	10 500.4	0.017	0.054	1.0(5.0)	j,k
		4	10 290.5	10 293.3	0.277	0.309	1.0(1.0)	e
		5	10 188.6	10 177.8	0.700	0.631	1.0(1.0)	e
	9/2	1	...	12 432.9	...	0.001	...	l
		2	...	12 086.0	...	0.017	...	
		3	...	11 786.8	...	0.123	...	k
		4	11 541	11 542.1	vw	0.403	1.0	j,k
		5	...	11 364.8	...	0.456	...	f,k
	5	1	...	13 766.2	...	0.2(-4)	...	l
		2	...	13 393.5	...	0.4(-3)	...	l
		3	...	13 065.5	...	0.006	...	f
		4	12 820(?)	12 787.1	vw	0.042	...	j
		5	...	12 566.0	w	0.199	...	m
		6	12 424	12 413.6	s	0.754	1.0	j
	11/2	1	...	15 088.3	...	0.8(-4)	...	l
		2	...	14 690.9	...	0.002	...	l
		3	...	14 335.7	...	0.019	...	l
		4	...	14 026.2	...	0.107	...	g
		5	...	13 767.6	...	0.332	...	g
		6	13 555(?)	13 565.8	...	0.541	...	n
	6	1	...	16 399.1	...	0.9(-6)	...	l
		2	...	15 977.8	...	0.3(-4)	...	l
		3	...	15 596.6	...	0.5(-3)	...	l
		4	...	15 258.2	...	0.005	...	
		5	14 963	14 966.0	w	0.029	1.0	o
		6	...	14 723.2	w	0.137	...	m
		7	14 514	14 515.6	s	0.829	1.0	o
	13/2	1	...	17 698.3	...	0.6(-5)	...	p
		2	...	17 254.0	...	0.2(-3)	...	
		3	...	16 847.9	...	0.002	...	g
		4	...	16 482.1	...	0.017	...	l
		5	...	16 159.1	...	0.084	...	
		6	...	15 880.3	...	0.271	...	f,k
		7	15 600(?)	15 637.0	...	0.625	...	j
	7	1	...	18 986.0	...	0.5(-7)	...	q
		2	...	18 519.3	...	0.2(-5)	...	q
		3	...	18 089.2	...	0.4(-4)	...	q
		4	...	17 697.4	...	0.4(-3)	...	q
		5	...	17 345.5	...	0.003	...	
		6	...	17 034.1	...	0.020	...	g
		7	...	16 756.8	...	0.104	...	g
		8	16 481	16 484.3	...	0.872	1.0	k

TABLE II (continued).

State	N	j	$\tilde{\nu}_j^{\text{obs}}(\text{cm}^{-1})$	$\tilde{\nu}_j^{\text{calc}}(\text{cm}^{-1})$	g_j^{obs}	g_j^{calc} ^b	Weights ^c	Notes
15/2	7	...	17 874	...	0.23	
	8	...	17 576	...	0.69	r
8	8	...	18 662	...	0.085	r
	9	...	18 320	...	0.90	r

^a Calculated values from the fit parameters in Table III. For further details refer to Table III and text. All states have *a'* symmetry.

^b The number in parentheses indicates the power of 10 (i.e. $0.9(-4) = 0.9 \times 10^{-4}$).

^c This column gives the weights for all those experimental values which were included in the fit. The number gives the weight for the corresponding frequency, the number in parentheses has to be multiplied by 10 000 to get the weight for the corresponding intensity. The factor arises from the different orders of magnitude of g_j and $\tilde{\nu}_j$ values that were included in the fit.

^d For our components (1/2)₁, (1)₁, and (1)₂ Ref. 16 gave 1387 (*AB* contour), 2820 (*B*) and 2720 cm⁻¹ (*B*) Ref. 20 gave 1380/1400 (*B*), 2812 (*A*), and 2706/2727 cm⁻¹ (*B*), and Ref. 21 gave 2843 and 2746 cm⁻¹ (in solution at 83 K).

^e Overlapping neighboring components; g_j^{obs} values are very approximate only.

^f Region superimposed by several weak bands, not assigned so far.

^g Region superimposed by H₂O lines.

^h For our components (2)₂ and (2)₃ Ref. 21 found 5487 and 5386 cm⁻¹, respectively (in solution at 85 K).

ⁱ Strongly overlapping with neighboring band; g_j^{obs} value very approximate only.

^j Band with a complex structure (unresolved rotational envelope. PQR or PQQR, respectively).

^k Poor signal to noise ratio.

^l Region superimposed by components of the next higher polyad.

^m Shoulder.

ⁿ Absorption with a complex structure. The minimum lies at about 13 522 cm⁻¹, the higher frequency maximum (listed) at 13 555 cm⁻¹. (Actually, one does not expect a resolved rotational envelope here).

^o Broad, unstructured band.

^p Out of frequency range.

^q Polyad overlap in the predicted band positions.

TABLE III. Parameters of the model Hamiltonian for CD₃CHO.

Parameter ^a	Fit 1 ^f	Fit 2 ^g
$\tilde{\nu}_s^{\text{c}}$ (cm ⁻¹)	2821.99	2825.67
$\tilde{\nu}_b^{\text{c}}$ (cm ⁻¹)	1402.17	1399.31
x_{sb}^{c} (cm ⁻¹)	- 65.86	- 66.48
x_{sb}^{c} (cm ⁻¹)	32.01	- 31.74
x_{bb}^{c} (cm ⁻¹)	- 6.82	- 6.55
k_{sbb}^{c} (cm ⁻¹)	± 92.89 ^b	± 93.31
n_v^{c}	22	22
n_g^{d}	9	9
R.m.s.(cm ⁻¹) ^e	4.44	4.22

^a All parameters are in cm⁻¹ units. 1 cm⁻¹ corresponds to 11.962 66 Jmol⁻¹.

^b The sign of k_{sbb} is undetermined.

^c Number of experimental band positions included in the fit.

^d Number of experimental g_j values (relative intensities) included in the fit.

^e Root mean square deviation for the n_v assigned bands of the CH chromophore.

^f Weight for all data included in the fit according to Table II.

^g Tenfold weight for the band center of the bending fundamental, unit weight for all other data, except intensities, see Table II.

TABLE IV. Integrated and summed band strengths for the polyads with integer *N* of the CH chromophore.^a

<i>N</i>	G/fm ²
1	670 000 ± 50 000
2	599 ± 160
3	219 ± 40
4	22 ± 2
5	1.43 ± 0.16
6	0.41 ± 0.08
7	0.041 ± 0.008

^a 95% confidence intervals are given for three to five separate measurements. See also the error discussion in the text.

from the two fits with two very different weights for the accurately measured and apparently unperturbed bending fundamental. Note in particular the very large value for $|k'_{sbb}| = 93 \text{ cm}^{-1}$, which is estimated to be accurate to within better than 10% including many possible error sources. This anharmonic coupling constant is thus larger than the diagonal anharmonicity constant x'_{ss} . It is of the same order of magnitude as found for the sp³ CH chromophore.⁴⁻¹⁰ In a time-dependent description, the large coupling leads to energy redistribution between the CH stretching and the in-plane bending motion on a subpicosecond time scale (about 0.1 ps).

Table IV summarizes the absolute intensities, summed for each polyad. We note a sharp drop in intensity at $N = 2$. Although this is established with certainty, the interpretation is not yet firm. The 95% confidence intervals are only part of the total error, which is estimated to be within 20% to 40% for the FTIR spectra (see Sec. II). The estimated values for $N > 5$ are given as an indication only, without any error limit (the error may be very large). The intensities of

TABLE V. Assignment of bands involving the CO stretching vibration (ν_4).

$\tilde{\nu}(\text{cm}^{-1})$	Assignment	Remarks
1754	$\nu_4(1752)^{\text{b}}$	
3138	$(\frac{1}{2} + \nu_4)_1(?)$	PQQR
3476	$2\nu_4(3478)^{\text{b}}$	Complex structure
4471	$(1 + \nu_4)_2$	PQQR
4552	$(1 + \nu_4)_1$	Complex structure
4855	$(\frac{1}{2} + 2\nu_4)_1(?)$	PQQR
5178	$3\nu_4(5178)^{\text{b}}$	c
5650-6000	$(3/2 + \nu_4)_{1,2} (?)$	Complex structures
6191	$(1 + 2\nu_4)_2$	PQQR
6281	$(1 + 2\nu_4)_1$	Complex structure
6865	$4\nu_4(6852)(?)^{\text{b}}$	Very weak, a,c
7076	$(2 + \nu_4)_3$	PQQR,c
7167	$(2 + \nu_4)_2$	PQQR,c
7345	$(2 + \nu_4)_1$	PQQR,c
7530	$(3/2 + 2\nu_4)_2(?)$	Complex structure
7680	$(3/2 + 2\nu_4)_1(?)$	Shoulder
8315-8385	$3_1(?)$	c
9854	$(3 + \nu_4)_2$	Absorption from 9790 to 9990

^a This region is also overlapped by the (5/2) polyad.

^b The numbers in parentheses are calculated for a Morse oscillator using $2\nu_4$ and $3\nu_4$ to determine $\tilde{\nu}_{\text{CO}} = 1765 \text{ cm}^{-1}$ and $x_{\text{CO}} = 13 \text{ cm}^{-1}$.

^c Overlapped by H₂O absorption lines.

the high overtones are of the same order of magnitude but somewhat larger than those found for the alkyl CH-chromophore.²⁸ Because of the experimental uncertainties, we have not pursued a theoretical evaluation.

In the high overtone region, most of the intensity is carried by the CH stretch–bend polyads. There is, in particular, no evidence for further Fermi resonance coupling with the low frequency out of plane CH bending or related vibrations. These seem to be adiabatically decoupled, at least on a short time scale. In the lower part of the spectrum, some further bands appear that can be associated with the CO stretching vibration and its combinations with the CH chromophore polyads.

D. Assignment of bands involving the CO stretching and other vibrations

Almost all of the intensity in the overtone spectrum can be accounted for by CH chromophore transitions and by CO overtones and combinations with the former. Many of these bands have been assigned in Table V. There we use the notation for combination polyads ($N + \nu_4$)_{*j*}, similar to simple polyads. The situation is quite similar to the combination polyads in CHF₃, CHD₃, and CHClF₂, where the relevant heavy atom vibrations are the CF₃-stretching and the CD₃-stretching vibrations, etc. Combinations with heavy atom vibrations involving the carbon atom of the CH chromophore seem to appear rather regularly. The matter has already been discussed in,^{7,9} but we have not found sufficient evidence for inclusion of an explicit coupling term in the effective Hamiltonian.^{7,9,29} The two band systems (with and without the heavy atom motions) can be analyzed as separate, effectively decoupled systems, although in the future perhaps a global analysis will become possible. Table V contains also the assignment of the CO stretching overtone series. This can be well fitted by a local Morse oscillator term formula up to $4\nu_4$. The coupled nature of the CO stretching and CH bending modes can be seen from the rotational band shapes. The pure local CH bending polarization is parallel to the *a* axis, giving much *A*-type band structure, whereas CO stretching is closer parallel to the *b* axis, giving *B*-type bands. In reality, the bands are hybrids whose description differs from a “local mode” interpretation.

IV. CONCLUSIONS

We can draw the following main conclusions:

(i) For the first time it has been possible to characterize completely the strong stretch–bend Fermi resonance in the overtone spectrum of an isolated CH chromophore of a sp² carbon atom. It is found that only the high frequency in-plane CH bending vibration participates in the anharmonic resonance system, whereas the out-of-plane CH bending frequency is adiabatically decoupled.

(ii) The effective anharmonic coupling parameter k'_{sb} has a large value (about 93 cm⁻¹ for CD₃CHO), similar to couplings found for the alkyl CH chromophore.^{4–10} This strong coupling results in a time scale of about 0.1 ps for energy flow between the CH stretching and bending vibrations.

(iii) Any further fine structure arising from coupling to other vibrations was not identified and is either much narrower or much less intense, corresponding to redistribution times at least an order of magnitude longer than for CH stretching and bending or to much less complete redistribution.

(iv) Overtones up to $\nu = 4$ for the CO stretching vibration and combination bands with the CH stretch bend system can be identified. The two band systems can be well analyzed separately and thus the coupling, if any, is off resonant.

This study also suggests some directions for future research. A more complete theoretical treatment might involve the CHO chromophore as a whole. The present results also pave the way for an inclusion of Fermi resonance in the analysis of overtone spectra of ordinary acetaldehyde (CH₃CHO), which so far has not been possible.¹⁷ This may prove crucial for a proper understanding of McKean's correlations between CH stretching frequencies and dissociation energies in this molecule.³⁰ A more detailed understanding of the physical significance of the Fermi resonance coupling in terms of the potential surface for acetaldehyde can be obtained by a combination with accurate *ab initio* calculations, which are well in reach for this molecule, similar to CHD₃.⁷ On a somewhat simpler level one can also use appropriate modifications of internal coordinate Hamiltonians for modeling the sp² CH stretch bend Fermi resonance.^{14,31,32} In this context, our results may also be helpful in the analysis of the more complex and so far not quantitatively understood spectra of the local sp² CH chromophore in benzene.^{13–15}

ACKNOWLEDGMENT

We are greatly indebted to G. Grassi for help with the synthesis of CD₃CHO and to T. Vettiger for taking NMR spectra. Y. Brunschweiler edited the manuscript. Financial support of our work by the US (under NSF CHE 85-05926) and Swiss National Science Foundations is gratefully acknowledged.

¹E. Fermi, *Z. Phys.* **71**, 250 (1931).

²Faraday Discussion on *Intramolecular Kinetics*, Faraday Disc. Chem. Soc. **75** (1983).

³Faraday Symposium on Molecular Vibrations No. 23, *J. Chem. Soc. Faraday Trans. II*, **84** (1988).

⁴K. von Puttkamer, H. R. Dübal, and M. Quack, *Faraday Disc. Chem. Soc.* **75**, 197, 263 (1983).

⁵H. R. Dübal and M. Quack, *Chem. Phys. Lett.* **80**, 439 (1981); *J. Chem. Phys.* **81**, 3779 (1984).

⁶S. D. Peyerimhoff, M. Lewerenz, and M. Quack, *Chem. Phys. Lett.* **109**, 563 (1984).

⁷M. Lewerenz and M. Quack, *J. Chem. Phys.* **88**, 5408 (1988).

⁸J. Baggott, M.-C. Chuang, R. N. Zare, H.-R. Dübal, and M. Quack, *J. Chem. Phys.* **82**, 1186 (1985).

⁹J. Segall, R. N. Zare, H. R. Dübal, M. Lewerenz, and M. Quack, *J. Chem. Phys.* **86**, 634 (1987).

¹⁰A. Amrein, H. R. Dübal, and M. Quack, *Mol. Phys.* **56**, 727 (1985); (to be published).

¹¹H. R. Dübal and M. Quack, *Chem. Phys. Lett.* **90**, 370 (1982).

¹²T. Carrington, Jr., *J. Chem. Phys.* **86**, 2207 (1987).

¹³E. L. Sibert, W. P. Reinhardt, and J. T. Hynes, *Chem. Phys. Lett.* **92**, 455 (1982); *J. Chem. Phys.* **81**, 1115 (1984).

¹⁴R. G. Bray and M. Berry, *J. Chem. Phys.* **71**, 4909 (1979).

¹⁵R. H. Page, Y. R. Shen, and Y. T. Lee, *J. Chem. Phys.* **88**, 4621 (1988).

- ¹⁶H. Hollenstein and Hs.H. Günthard, *Spectrochim. Acta A* **27**, 2027 (1970), and earlier references quoted there.
- ¹⁷L. A. Finsen, H. L. Fang, R. L. Swofford, and R. R. Birge, *J. Chem. Phys.* **84**, 16 (1985).
- ¹⁸R. Nakagaki and I. Hanazaki, *Chem. Phys. Lett.* **128**, 432 (1986).
- ¹⁹R. W. Kilb, C. C. Lin, and E. B. Wilson, Jr., *J. Chem. Phys.* **26**, 1695 (1957).
- ²⁰R. J. Capwell, Jr., *J. Chem. Phys.* **49**, 1436 (1968).
- ²¹G. Lucazean and C. Sandorfy, *Can. J. Chem.* **48**, 3694 (1970).
- ²²J. S. Crighton and S. Bell, *J. Mol. Spectrosc.* **112**, 285, 304, 315 (1985).
- ²³J. C. Morris, *J. Chem. Phys.* **11**, 230 (1943).
- ²⁴A. J. Bauder, F. J. Lovas, and D. R. Johnson, *J. Phys. Chem. Ref. Data* **5**, 53 (1976).
- ²⁵D. W. Chandler, W. E. Farneth, and R. N. Zare, *J. Chem. Phys.* **77**, 4447 (1982).
- ²⁶M.-C. Chuang, J. E. Baggott, D. W. Chandler, W. E. Farneth, and R. N. Zare, *Faraday Disc. Chem. Soc.* **75**, 301 (1983).
- ²⁷H. H. Nielsen, *Rev. Mod. Phys.* **23**, 90 (1951), *Handbuch Phys.* **37** (1959); G. Amat, H. H. Nielsen, and G. Tarrago, *Rotation Vibration of Polyatomic Molecules* (Marcel Dekker, New York, 1971).
- ²⁸A. Amrein, H. R. Dübal, M. Lewerenz, and M. Quack, *Chem. Phys. Lett.* **112**, 387 (1984).
- ²⁹J. E. Baggott, D. W. Law, and I. M. Mills, *Mol. Phys.* **61**, 1309 (1987).
- ³⁰D. C. McKean, *Chem. Commun.* **21**, 1373 (1971).
- ³¹J. S. Wong, W. H. Green, W. D. Lawrance, and C. B. Moore, *J. Chem. Phys.* **86**, 5994 (1987); W. H. Green, W. D. Lawrance, and C. B. Moore, *ibid.* **6000** (1987).
- ³²T. Carrington, L. Halonen, and M. Quack, *Chem. Phys. Lett.* **140**, 512 (1987) (see also Ref. 3, p. 1371).